Mon. Not. R. astr. Soc. (1992) **256,** 655–668

H0414 + 009 – an X-ray bright BL Lac with a radio tail in a distant cluster of galaxies

I. M. McHardy,[1]★† G. A. Luppino,[2]†‡ I. M. George,[3]★§ R. G. Abraham[4]¶ and B. A. Cooke[5]†

[1] *Department of Physics, University of Southampton, Southampton SO9 5NH*
[2] *Institute for Astronomy, University of Hawaii, Honolulu, Hawaii 96822, USA*
[3] *Institute of Astronomy, Madingley Road, Cambridge CB3 0HA*
[4] *Department of Astrophysics, University of Oxford, Oxford OX1 3RH*
[5] *Department of Physics, University of Leicester, Leicester LE1 7RH*

Accepted 1992 January 6. Received 1991 November 21

SUMMARY

VLA observations of the X-ray selected BL Lac H0414 + 009 at 6, 20 and 90 cm show that it has a steep-spectrum ($\alpha \simeq 1$; $f_\nu \propto \nu^{-\alpha}$) radio tail. The tail extends ~40 arcsec from the core, in a gentle curve. There is no evidence of extended emission on the opposite side of the core. This is by far the clearest example of a single-sided radio tail associated with a BL Lac source. The low radio luminosity (1.6×10^{25} W Hz^{-1} at 20 cm for $H_0 = 50$ km s^{-1} Mpc^{-1} and $q_0 = 1/2$ at $z = 0.287$) and morphology of the extended emission strengthens the proposed association of BL Lacs with Fanaroff–Riley type I (FR I) radio sources.

Deep *V*, *R* and *I* CCD images show that the BL Lac is located in a galaxy whose surface brightness and colours are best fitted by an elliptical model with absolute total magnitude $M_V = -23.53$. The elliptical host galaxy is the brightest of a poor cluster. We confirm the recently published redshift ($z = 0.287$) for the BL Lac and find similar redshifts for five of the surrounding, faint galaxies, supporting the conclusion that the BL Lac and the cluster are physically associated and are not merely a chance superposition. We conclude, contrary to earlier suggestions, that BL Lacs do not avoid the cluster environment but are found in groups and clusters just as often as are normal radio galaxies, consistent with the hypothesis that BL Lacs are simply normal radio galaxies seen 'end-on'.

The appearance of the cluster is striking, containing a number of 'twin' galaxy pairs. It has been suggested that the pairs could be the result of gravitational lensing by a foreground cosmic string, but our observations do not support this hypothesis.

We have analysed the cluster properties and present *VRI* CCD photometry for 108 galaxies fainter than the BL Lac host galaxy in the CCD images (1.1×1.2 Mpc^2). In the Bautz–Morgan morphological classification scheme we classify this cluster as BM I. The cluster could be as rich as Abell class 0, however, the richness may be lower due to considerable uncertainties in the corrections for the field galaxy background and the small field of view of the CCD.

We have searched deep *EXOSAT* images for evidence of extended X-ray emission from a hot intracluster medium, but find none. The upper limit to the luminosity of

★Visiting Astronomer, Very Large Array (VLA), National Radio Astronomy Observatories, operated by AURA under contract with the National Science Foundation.
†Observer, 2.4-m telescope, Michigan–Dartmouth–MIT (MDM) Observatory.
‡Visiting Astronomer, KPNO 4-m telescope, National Optical Astronomy Observatories, operated by AURA under contract with the National Science Foundation.

§Present Address: Laboratory for High Energy Astrophysics, Code 668, NASA/Goddard Space Flight Center, Greenbelt, MD 20771, USA.
¶Present Address: Dominion Astrophysical Observatory, National Research Council of Canada, Herzberg Institute of Astrophysics, 5071 West Saanich Road, Victoria, BC, V8X 4M6, Canada.

any cluster-type emission from 0414+009, however, is still rather high, $L_x(2\text{–}10\ \text{keV}) \leq 4 \times 10^{37}$ W, comparable with that of moderately X-ray luminous Abell clusters. If hot gas emitting at that luminosity does exist in the cluster, it could help explain the unusual structure of the radio source.

Key words: BL Lacertae objects: individual: H0414+009 – galaxies: clustering – radio continuum: galaxies – X-rays: galaxies.

1 INTRODUCTION

The remarkable properties (rapid variability, high polarization, featureless optical spectra, etc.) of BL Lacertae objects (BL Lacs) are well known. The most widely accepted explanation of BL Lacs is the 'unified scheme' for AGN (e.g. Browne 1989), in which it is proposed that we are observing a subclass of 'normal' radio galaxies whose relativistic jets lie nearly along our line of sight. It has also been proposed, however, that we may be observing distant quasars that are gravitationally microlensed by a foreground galaxy (Ostriker & Vietri 1985). Recently, it has become clear that deep optical imaging may help us understand these objects. For example, imaging of the host galaxies of BL Lac objects (McHardy *et al.* 1991; Abraham, McHardy & Crawford 1991) reveals that the BL Lac cores always lie exactly in the centre of the host galaxies, arguing against the lensing model.

Additional information can be gleaned from the study of the environments of BL Lacs. If the unified scheme is correct then we expect to find the same percentage of BL Lacs in clusters as we find of normal double radio sources in clusters. So far, the subject of the BL Lac environments has received little attention, although it has been suggested that BL Lacs may avoid a rich-cluster environment (Weistrop *et al.* 1981). In this paper we present a multiwaveband study of the unusual BL Lac 0414+009 and its environment, which is very relevant to these considerations.

The X-ray source 1H0414+009 was discovered by Ulmer *et al.* (1980) in a *HEAO1-A1* observation of the distant cluster of galaxies Abell 480. Subsequent observations with the *Einstein* IPC and HRI (Ulmer *et al.* 1983) showed that the source was point-like (<3 arcsec), coincident with a 16th mag stellar object, and thus not identified with A480. Radio and optical observations confirmed that the identification was a BL Lac.

Luppino (1989) presented deep CCD images showing that the BL Lac was surrounded by a distant cluster of galaxies. Recently, Halpern *et al.* (1991) determined a redshift of $z=0.287$ for the BL Lac itself, while Falomo, Melnick & Tanzi (1990) and Falomo & Tanzi (1991) indicated that the BL Lac might lie in an elliptical host galaxy, and noted the surrounding cluster of galaxies initially reported by Luppino (1989). Furthermore, based on the large number of possible 'twin' galaxies present in the field, Falomo, Tanzi & Treves (1991) speculated that 0414+009 might be gravitationally lensed by a foreground cosmic string.

In Section 2 we discuss our VLA radio observations which show that the BL Lac exhibits a steep-spectrum radio tail as well as a compact core. We present 6-, 20- and 90-cm data including polarization, spectral and variability measurements. Our optical observations are described in Section 3. Here we present our own *V*, *R* and *I* CCD images which go much deeper than those of Falomo & Tanzi (1991) and Falomo *et al.* (1991), and confirm that the BL Lac lies in an $R \simeq 17.5$ host galaxy which is the brightest member of a distant cluster of galaxies. Detailed profile fitting of the subarcsec CCD images indicates that the host galaxy is elliptical. In addition to the imaging data, we present spectroscopic observations of the BL Lac and some of the surrounding galaxies. We also discuss the possibility that some of the faint galaxies in the 0414+009 field are gravitationally lensed by a cosmic string. In Section 4 we discuss our search for extended X-ray emission from an intracluster medium whose existence is implied by the distorted radio morphology. Finally, in Section 5, we summarize our results, and their implications for the 'unified theory' of BL Lacs.

2 RADIO OBSERVATIONS

We observed 0414+009 briefly with the VLA on five occasions between 1984 July and 1985 August as part of a monitoring programme. Even in these short observations it was clear that extended emission, in the form of a tail, was present over and above emission from the core. (A low-resolution map, very similar to one of our early maps, is shown by Schmelz, Feigelson & Schwartz 1986.) Detailed observations were therefore made on 1987 September 9 to clarify the morphology of the extended structure using the VLA in A array. The source was observed for 97 min at 6 cm, 135 min at 20 cm, and 139 min at 90 cm. The data were calibrated and mapped in the usual way, applying phase self-calibration to the data and CLEANing the maps. These observations are discussed below. The 20-cm observations are the deepest and so these are discussed in more detail. All of the radio observations are recorded in Table 1.

2.1 20-cm observations

The 20-cm map (Fig. 1) shows an unresolved core from which extends a jet-like structure of low surface brightness.

Table 1. Summary of VLA radio observations.

Date	Wavelength	Observation Time (mins)	Flux Density Core(mJy)	Flux Density Tail(mJy)	Comments
10 Jul 1984	20 cm	~ 5 – 10	100	20	**
05 Nov 1984	20 cm	~ 5 – 10	85	45	**
12 Jan 1985	20 cm	~ 5 – 10	70	20	**
22 Apr 1985	20 cm	~ 5 – 10	85	35	**
05 Aug 1985	20 cm	~ 5 – 10	73 ± 5	40 ± 10	
10 Jul 1984	6 cm	~ 5 – 10	42	8	**
22 Apr 1985	6 cm	~ 5 – 10	60	5	**
05 Aug 1985	6 cm	~ 5 – 10	57 ± 5	10 ± 3	
09 Sep 1987	6 cm	97	57 ± 2	10 ± 3	small tail
09 Sep 1987	20 cm	135	75 ± 2	40 ± 5	tail obvious
09 Sep 1987	90 cm	139	52 ± 10	150 ± 50	noisy map

**Flux densities estimated from visibility plots, sometimes from partial arrays. Typical errors are around 10 mJy.

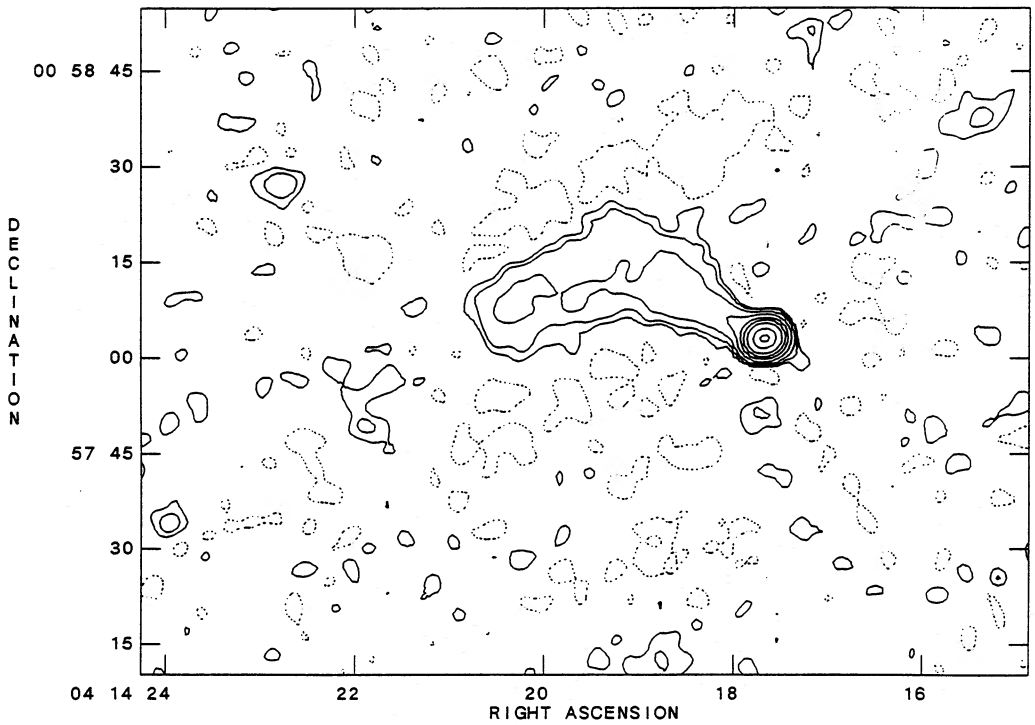

Figure 1. 20-cm VLA radio map. The peak flux density is 75.6 mJy beam^{-1} and the contours are at −0.15, 0.15, 0.3, 0.7, 2, 5, 10, 20, 50 and 90 per cent of the peak.

The rms noise level in this map is 0.06 mJy beam^{-1}. The jet leaves the core at position angle ~60°. At its apex the jet appears unresolved but opens out with an opening angle of ~35°. Approximately 10 arcsec from the core it broadens into a diffuse structure and bends around gradually to position angle 100°. The total length of the structure is ~40 arcsec corresponding to a metric size of ~220 kpc at the redshift of the cluster (5.4 kpc arcsec^{-1} at $z=0.287$; for the remainder of this paper we adopt a cosmology with $H_0=50$ km s^{-1} Mpc^{-1}, $q_0=1/2$ and $\Lambda=0$ unless otherwise noted).

The source has some similarities to the radio-tail sources found in clusters of galaxies (e.g. M^{c}Hardy 1979), but our observations show no evidence for the twin tails usually seen in such sources. There is a hint of a possible (~1 arcsec) elongation from the core on the opposite side from the jet, but this is close to the noise level of the map and is probably not real. We also note that there is no evidence for any large-scale extended emission to the west of the core. Thus, although the lack of a counter-jet can be easily explained by relativistic beaming effects, the lack of symmetrical extended emission which would not be beamed indicates that the source is probably an intrinsically single-sided jet.

Radio maps of BL Lacs generally show low-level diffuse structure surrounding a compact core, although some cases of double-lobed emission are known (e.g. Antonucci & Ulvestad 1984; Wardle, Moore & Angel 1984). Only two possible cases of radio-tail BL Lac sources are known, PKS0548−322 (Antonucci & Ulvestad 1984) and 1400+162 (Hintzen & Owen 1981), although morphological classification is sometimes difficult as dynamic range problems limit the ultimate map sensitivities. To the best of our knowledge this is the only example of a large, well-resolved, single-sided radio tail, or jet. Its morphology is that of Fanaroff–Riley class I (Fanaroff & Riley 1974). The flux density of the radio tail is ~40 mJy at 20 cm, corresponding to a luminosity of 1.6×10^{25} W Hz^{-1}. This is below the dividing luminosity between FR I and FR II radio sources (~5×10^{25} W Hz^{-1} at 20 cm) and so is again consistent with FR I classification.

The radio core is coincident with the *Einstein* HRI position of H0414+009 and with the position of the optical counterpart which is located at 1950.0 coordinates $04^{h}\ 14^{m}\ 17\overset{s}{.}6$, +00° 58′ 03″.4 (Ulmer *et al.* 1983). The core flux at 20 cm is 75±2 mJy. Thus the core/extended flux ratio is ~1.9, which, although higher than the average for normal extragalactic sources (~0.1) is on the low side for blazars (~10; Wardle *et al.* 1984).

A second source located at $04^{h}\ 14^{m}\ 11\overset{s}{.}0$, +00° 58′ 22″ (1950) roughly 18.6 arcsec north and 99 arcsec west of the BL Lac) was detected in our 20-cm observations. However, this appears to be a background double source and has no obvious optical identification on the Palomar Sky Survey. The source is just off the edge of our CCD images.

2.2 90- and 6-cm observations

Self-calibration of the 90-cm data base proved difficult and the resultant map is very noisy (noise level ~4 mJy beam^{-1}). The 90-cm map therefore does not show the same detail as the 20-cm map, and so we do not present it here, but it confirms the same basic structures of an unresolved core and extended low surface brightness region stretching ~1 arcmin to the east. The core flux density is very approximately 52±10 mJy and the flux in the tail is very approximately 150±50 mJy.

The 6-cm map (again, not shown here) reveals only a very small tail (~2 arcsec) extending from a bright core in posi-

tion angle ~ 60°. The total flux density in the tail is ~ 10 mJy and in the core is 57 ± 2 mJy.

2.3 Radio polarization

The 20-cm observations were calibrated for polarizations using 3C286 as the polarization calibrator. The low signal in the extended emission prevents detection of polarization there, but polarized flux is detected from the core. The level, however, is not high. The peak polarized flux density is 1.53 ± 0.1 mJy (i.e. 2 per cent). There is also a hint of polarized emission from the base of the jet. The low polarization may be related to the low ratio of core-to-extended flux and the lack of noticeable radio variability (see Section 2.5) and may indicate that the radio emission in 0414 + 009 is not beamed closely to our line of sight.

The 6-cm observations were also calibrated for polarization using 3C286 as the calibrator. Unresolved polarized emission is detected from the core with a peak flux density of 1.56 ± 0.1 mJy, almost identical to the polarized flux from the core at 20 cm, but of higher percentage polarization (2.7 per cent). The position angle of the *E*-vector in the 6-cm core is ~ 3°. However at 20 cm the position angle of the *E*-vector in the core is 50°. This is very close to the position angle of the arcsecond-scale jet as it leaves the core. It has been noted by Rusk (1988) that, in BL Lacs, the radio *E*-vector generally lies parallel to the VLBI structural axis. In this context we would propose that in 0414 + 009 the radio jet initially leaves the core close to position angle ~ 3° and then bends round to ~ 50° farther out. Variations in optical depth prevent us from detecting significant polarized flux from very close to the core at lower frequencies (i.e. at 20 cm). Similar bending jets and optical depth effects are commonly seen in VLBI observations of blazars (e.g. McHardy *et al.* 1990).

2.4 Spectral index of the core and the tail

The above observations allow determination of the overall spectral index of the core and of the tail separately. The core has the flat spectrum ($\alpha \simeq 0.15$ defined in the sense $f_\nu \propto \nu^{-\alpha}$) usually seen in BL Lacs, while the tail has a steep spectrum with $\alpha \simeq 1$. The tail appears somewhat shorter at 5 GHz which is probably a surface brightness effect but may also indicate some spectral steepening with increasing distance from the core. These spectral indices are entirely typical of extragalactic radio sources in general and add further weight to the 'unified scheme'.

2.5 Radio variability

In Table 1 we have listed the fluxes derived from all our observations, including the short monitoring observations which were carried out in a number of different array configurations, often with only part of the whole array. In many cases the fluxes are derived from examination of the visibility plots alone. In these cases the estimate of the core flux, determined at long baselines, is more accurate than that of the extended emission, determined at short baselines where confusing sources are more of a problem. We can see that there is little or no evidence for any variability. We also note that the derived flux densities are similar to those listed by Ulmer *et al.* (1983) from observations on 1981 October 26 (101 mJy at 1.4 GHz; 83 mJy at 5 GHz) which they quote as arising from a point source (beamsize 8.4 arcsec at 1.4 GHz). Ulmer *et al.* (1983) make no mention of the extended structure which we see. The lack of significant variability supports the view that the core radio emission may not be highly beamed.

3 OPTICAL OBSERVATIONS

3.1 CCD imaging

Following our VLA discovery of the radio tail in 1985, we imaged the field containing 0414 + 009 with the 2.4-m Hiltner telescope at the MDM Observatory on various occasions in 1986 and 1987. We detected extended emission underlying the BL Lac itself and discovered the surrounding cluster of galaxies. Unfortunately we were never able to obtain images in very good seeing, so we were unable to attempt discrimination between an elliptical or disc host. In 1989 March, however, we acquired excellent CCD images of the 0414 + 009 field in subarcsecond seeing (0.8–0.9 arcsec FWHM) using the TI-2 800 × 800 CCD at the prime focus of the Kitt Peak 4-m telescope. All the following analysis is based on these high-quality data.

The scale of the 4-m images was 0.29 arcsec per pixel resulting in a field of view of 3.87 × 3.87 arcmin^2. Observations of Landolt standard stars (Landolt 1983) indicated that the night was photometric. Our filter bandpasses, combined with the CCD sensitivity, provide a good approximation of Johnson *V* and Kron–Cousins *R* and *I* bands, and our photometric calibration on these standard systems is given by the following equations:

$$V = -2.5 \log kf_{\mathrm{ADU/s}} + 26.149 - 0.07(V-I) - 0.15 \sec z,$$

$$R = -2.5 \log kf_{\mathrm{ADU/s}} + 25.791 - 0.04(V-I) - 0.05 \sec z,$$

$$I = -2.5 \log kf_{\mathrm{ADU/s}} + 25.415 - 0.07 \sec z,$$

where *k* is the CCD gain constant (4.15 e^- per ADU). Each observation was of 640 s duration. The images were flattened and cleaned of cosmic rays in the usual manner. Our observations confirm the existence of an extended galaxy underlying the BL Lac core, and a group of galaxies surrounding the BL Lac. The *R*-band image is shown in Plate 1 and a contour diagram of this image is shown in Fig. 2. A summary of these observations, as well as the spectroscopic observations described in a later section, are listed in Table 2.

3.1.1 *The host galaxy of H0414 + 009*

We have carefully analysed the surface brightness profile of the host galaxy of H0414 + 009 by fitting it to elliptical isophotes. In this case an eccentricity of ~ 0.1 provides the best fit. We used computer codes developed by R. Jedrzejewski (Jedrzejewski 1987) and based on the GASP surface photometry package of M. Cawson (Cawson 1983). The reader is referred to Abraham *et al.* (1991) for a more detailed discussion of this procedure.

We have separately analysed the *V*-, *R*- and *I*-band images and have fitted the resultant profiles of 0414 + 009 to combinations of an unresolved core and an elliptical host galaxy and an unresolved core and a disc host galaxy. The

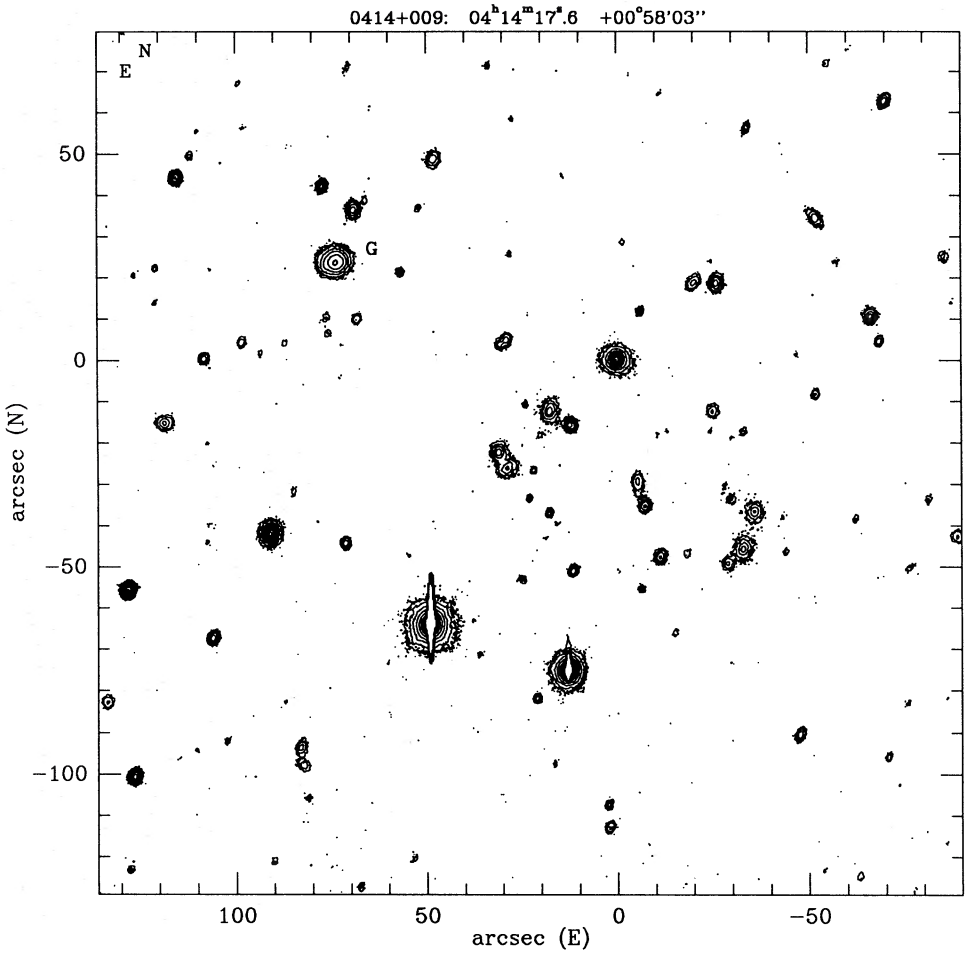

Figure 2. *R*-band contour map of the field containing 0414+009 and surrounding cluster. This shows the 720×780-pixel sub-image (3.5×3.8 arcmin^2) analysed by FOCAS.

Table 2. Summary of optical observations.

CCD Imaging

Observatory/Telescope	CCD	Pixel Scale	Filter	Seeing	Δt
KPNO 4m	TI 800 × 800	0″.29	*V*	0″.85	640 s
”	”	”	*R*	”	”
”	”	”	*I*	”	”

Spectroscopy

	Spectrograph	Å/pixel	Slit	Angle	Δt
MDM 2.4m	Mk III	5.14	2″.4	72.7°	6000 s
”	”	”	1″.7	126°	3236 s
”	”	”	1″.7	13°	5400 s
AAT	IPCS	2	2″.0	57°	3600 s
”	FORS	10.1	2″.0	57°	3600 s

profile fits to the *V*- and *R*-band images are shown in Figs 3 and 4 respectively. Point spread function (psf) stars were taken from the same image as the BL Lac profile. The fit to the *I*-band image is subject to possible uncertain errors as the psf star was slightly saturated in this image (this was not the case for the *V* or *R* images). Statistical tests reveal only a marginal preference for an elliptical host in all wavebands. However, visual examination of Figs 3 and 4 shows that, at radii larger than about 4 arcsec, the data are visually a better fit to an elliptical model. The inability of the statistical test to tell the difference arises because the overall fit is dominated by points at small radii where the core is by far the largest factor. We list the best-fitting parameters in Table 3. For the elliptical model, r_e is the radius in arcsec within which half the total light is emitted, and Σ_e is the surface brightness in mag arcsec^{-2} at r_e. For the disc model, r_s is the radius at the 1/e surface brightness contour and Σ_s is the central surface brightness. Uncertainties in the characteristic radii and surface brightnesses can be as large as 30 per cent and 0.2–0.3 mag arcsec^{-2} respectively. These errors have been estimated by Monte Carlo simulations (Abraham 1991; Abraham *et al.*, in preparation). From these fits we can determine total magnitudes (i.e. integrated out to infinity) and also magnitudes within various apertures such as the 32 kpc ($H_0=50$) diameter aperture often used for these studies (e.g. Luppino *et al.* 1991), as well as a 32 h_{60}^{-1} kpc diameter aperture used by Hoessel, Gunn & Thuan (1980; hereafter HGT) in their investigation of the brightest galaxies in Abell clusters. Here, the HGT aperture corresponds to a 3.5-arcsec radius and a 32-kpc ($H_0=50$) aperture corresponds to a 3.0-arcsec radius. (The difference between magnitudes measured in 3.0 and 3.5 arcsec radius apertures is very small, typically being

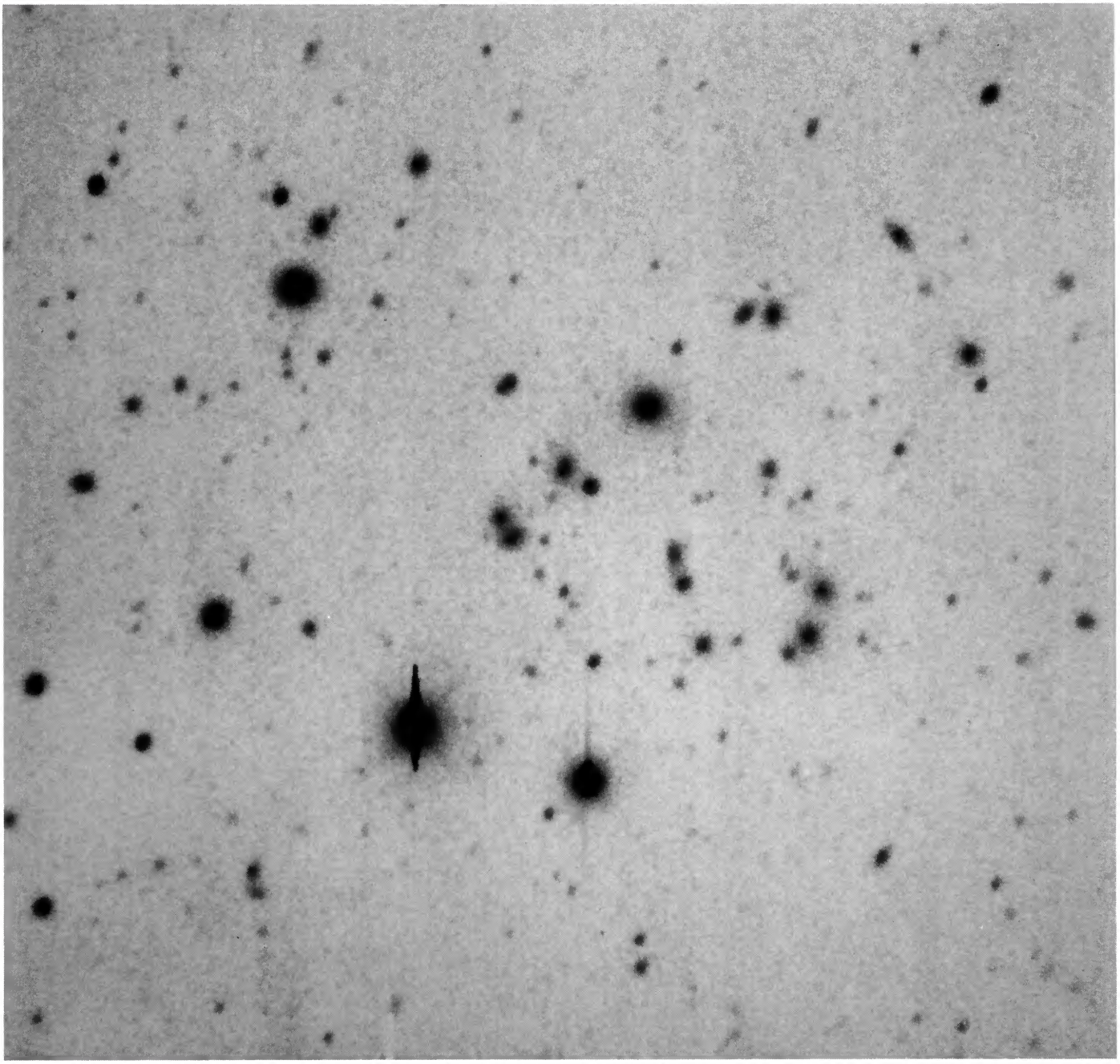

Plate 1. *R*-band CCD image. This 640-s exposure covers 3.87×3.87 arcmin^2 at 0.29 arcsec per pixel.

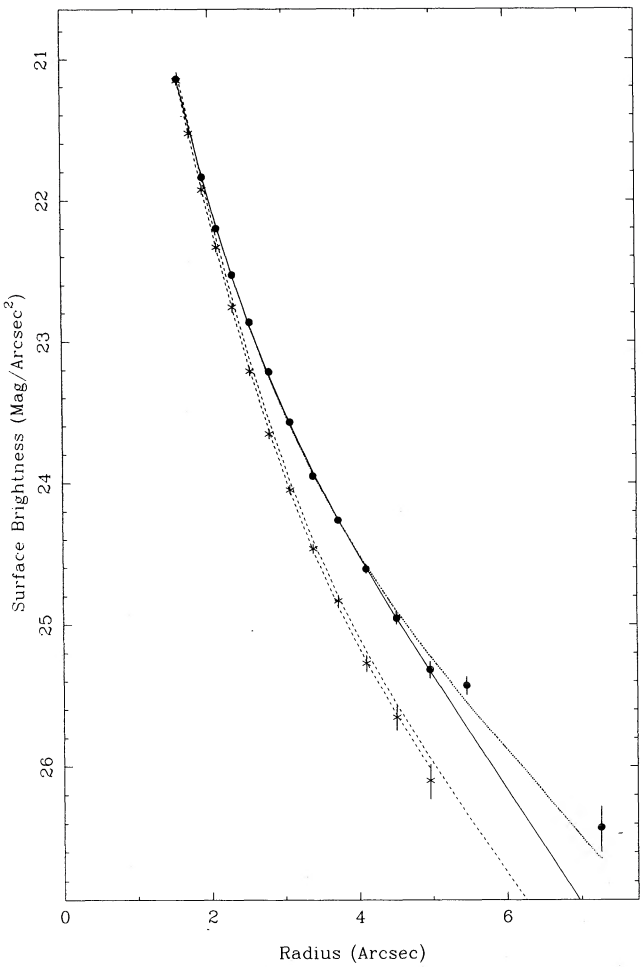

Figure 3. Model galaxy profile fits to the *V*-band image. The dots represent the data; the stars, which are joined by the lower dashed line, represent the stellar point spread function as observed and the upper dashed line shows the psf scaled to the maximum of the BL Lac profile. The solid line is the best-fitting disc galaxy model and the dotted line is the best-fitting elliptical galaxy model.

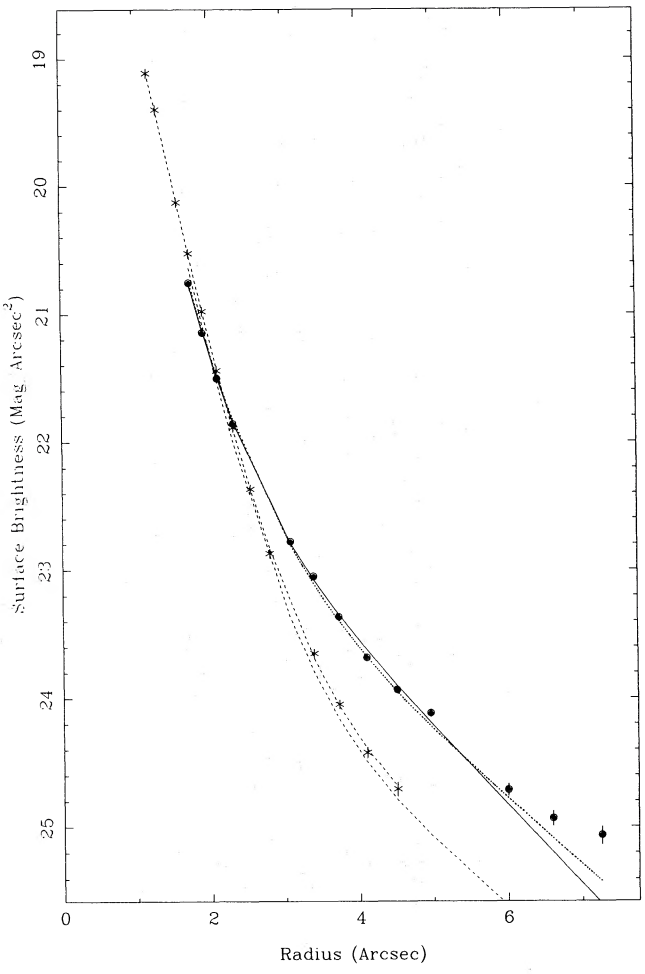

Figure 4. Model galaxy profile fits to the *R*-band image. The dots represent the data; the stars, which are joined by the upper dashed line, represent the stellar point spread function as observed and the lower dashed line shows the psf scaled to the maximum of the BL Lac profile. The solid line is the best-fitting disc galaxy model and the dotted line is the best-fitting elliptical galaxy model.

Table 3. BL Lac host galaxy models and model magnitudes.

	Elliptical Model $\Sigma(r) = \Sigma_e e^{-7.67[(r/r_e)^{1/4}-1]}$			Disc Model $\Sigma(r) = \Sigma_s e^{-r/r_s}$		
Waveband	model parameters	magnitudes Total	3" radius	model parameters	magnitudes Total	3" radius
V	$r_e = 1.28$ $\Sigma_e = 22.57$	18.56	19.10	$r_s = 1.23$ $\Sigma_s = 21.82$	19.38	19.87
R	$r_e = 1.47$ $\Sigma_e = 21.72$	17.49	18.00	$r_s = 1.55$ $\Sigma_s = 21.21$	18.26	18.98
*I**	$r_e = 1.23$ $\Sigma_e = 20.36$	16.52	16.96	$r_s = 1.40$ $\Sigma_s = 20.04$	17.31	17.93

*Saturated psf star.

only 0.05–0.1 mag. Total and 3.0 arcsec radius magnitudes are listed in Table 3.

We can compare the magnitudes of the host galaxy in the various wavebands with those of the surrounding galaxies and see that it is indeed the brightest galaxy in the cluster. The magnitudes of the other galaxies (also in a 3.0 arcsec radius aperture) are listed in Table 4(a) and the properties of the cluster galaxies are discussed in the next section.

For both elliptical and disc models $(V-R)_{\rm observed} \sim 1.1$, which, at a redshift of $z=0.287$, corresponds roughly to rest-frame $(B-V)$. The colours are therefore comparable with those of an early-type galaxy [$(B-V)_{\rm rf}=0.9$ for an elliptical or S0 galaxy but $(B-V)_{\rm rf}=0.5$ for an Sc galaxy]. Assuming a reddening of $A_V=0.48$ (Elvis, Lockman & Wilkes 1989) and a K-correction of $K_V=0.3$, the absolute total magnitude of the host galaxy is $M_V=-23.53$. Although this value of M_V is larger than the canonical value for the total absolute magnitude of $M_V=-22.5$ formerly assumed to be the norm for host galaxies of BL Lacs (e.g. Ulrich 1989), recent survey observations by Abraham *et al.* (1991) show that this larger M_V value is not particularly unusual. In their imaging study of a number of BL Lac host galaxies, Abraham *et al.* found $\langle M_V\rangle_{\rm Total}=-23.3$.

We note that the luminosity of the extended (and therefore unbeamed) radio emission in 0414+009 is more or less what we expect for an elliptical galaxy of this absolute magnitude (Colla *et al.* 1975).

Within the 3.5 arcsec radius (HGT) aperture, $M_V=-23.04$, comparable with that expected for the brightest galaxy in a cluster of richness class 0 (-23.05 converting HGT magnitudes hereafter to $H_0=50$, $q_0=0.5$ and averaging over all cluster morphological types).

Our observations essentially agree with those of Falomo & Tanzi (1991) who made a short (120 s) R-band exposure of 0414±009 with the ESO New Technology Telescope with ~0.9-arcsec resolution in 1989 August. They fitted their data to an elliptical model only and concluded that $r_e=0.8$ arcsec, $\Sigma_e=21.1$ and $m_R=17.8$, resulting in an absolute (presumably total) magnitude of $M_V=-23.2$. They claim that the BL Lac is located in the centre of the galaxy to within 0.1 arcsec. Our measurements confirm this claim and we note that in all other cases where sufficiently accurate location has been possible, the BL Lac cores are always centrally located in their host galaxies (Abraham *et al.* 1991), which is not expected in lensing models for BL Lacs (Ostriker & Vietri 1985, 1990).

Halpern *et al.* (1991) estimate that the absolute magnitude of the host galaxy is closer to $M_V \simeq -24$, implying that this galaxy is exceptionally bright ('one of the most luminous galaxies known' they claim). Neither our observations, nor those of Falomo & Tanzi (1991) support this conclusion, which is derived from deconvolution of a spectrum into a BL Lac power law and a standard elliptical galaxy, and which should therefore not be expected to be of high photometric accuracy.

3.1.2 *The surrounding cluster of galaxies*

Inspection of the CCD image shown in Plate 1 reveals an apparent cluster of galaxies, some of which are grouped in pairs, arranged around the BL Lac. Is this a case of a BL Lac whose host galaxy is a member of a distant cluster, or are we merely seeing an increased background galaxy density in this direction? In order to address this question, we obtained deep multicolour CCD images of the 0414+009 field and spectra of a number of the fainter galaxies. The CCD photometry is discussed in this section and the spectra in the following section. The group of galaxies surrounding the BL Lac has also been discussed by Falomo *et al.* (1991) who present a short exposure (120 s) covering 2.2×1.4 arcmin^2 (0.73×0.46 Mpc^2 at the cluster redshift). However, our data go at least 1–1.5 mag fainter and cover 1.1×1.2 Mpc^2, over four times the field of Falomo *et al.* at the same or better resolution (seeing FWHM < 0.9 arcsec). Moreover, we obtained our deep images in three colours (*VRI*).

Our initial 800×800-pixel CCD images were trimmed to 780×720 pixels before being analysed using the image analysis package FOCAS (Jarvis & Tyson 1981). The trimming was necessary to remove some saturated regions near the edge of the CCD. FOCAS photometered and classified all the objects in this subframe as stars (s), 'fuzzy' stars (sf), galaxies (g), extended (diffuse) objects, or noise depending on the shape of the objects as compared to the point spread function determined from bright stars in the field. Given the depth and resolution of our data, galaxies could be distinguished from stars down to a magnitude where virtually all the objects in the field were galaxies. Three FOCAS catalogues (*VRI*) were prepared and all the objects in the catalogues, especially those classified as diffuse or noise, were visually inspected to be certain they were real. Any spurious objects were removed from their respective catalogues. A common coordinate system was selected, centred on the BL Lac with offsets measured in arcsec, and the three catalogues were combined. The resulting matched catalogue contains 123 objects located at the same celestial coordinates in all three colours. Of these 123 objects, 15 were classified as stars in all three catalogues. Each of the remaining 108 objects were classified as a galaxy or a 'fuzzy' star in at least one of the 3 colours; these are listed in Table 4(a). In Table 4(b) we list the stellar objects. The object number (sorted by declination) is listed in column 1, followed by any interesting notes concerning that particular object in column 2. The offset coordinates (with respect to the BL Lac) are given in columns 3 and 4, and the classifications (as noted above) in each of the catalogues are listed in columns 5, 6 and 7. The remaining columns contain the aperture magnitudes and colours. As mentioned earlier, we used a 32 kpc diameter aperture (6 arcsec) consistent with similar studies of distant clusters.

Falomo *et al.* (1991) identify five pairs of galaxies labelled A to E, 1 and 2, which they speculate could be the result of lensing by a foreground cosmic string (Cowie & Hu 1987). We have listed these labels in Table 4(a) and show these galaxies in the *I*-band contour map (Fig. 5). Besides the pairs noted by Falomo *et al.* we can find quite a few more pairs over the field (we have added pair F to the list and show it in Fig. 5). The range of pair separations seen implies that, if these pairs are the result of lensing by a foreground cosmic string, the background lensed galaxies have a range of different redshifts (e.g. see Cowie & Hu 1987). We can also, however, identify many galaxies that are not in pairs. Although visually striking, we do not think there is much to be gained by speculation regarding the probability of such pairings occurring by chance. We prefer to trust spectral observations (described later), but note that if all the

Table 4. (a) *VRI* CCD photometry of the galaxy cluster surrounding the BL Lac H0414 + 009.

Obj	Notes	arcsec(E)	arcsec(N)	cl$V$	cl$R$	cl$I$	V	R	I	$V-R$	$R-I$	$V-I$
1		−63.20	−124.70	s	g	s	22.95	21.79	20.81	1.16	0.98	2.14
2		−53.90	−123.20	s	g	s	22.94	22.59	22.20	0.35	0.39	0.75
3		127.30	−123.20	g	s	g	22.36	21.91	21.60	0.44	0.31	0.75
4		−17.10	−121.50	s	g	g	24.54	23.71	22.78	0.83	0.93	1.76
5		89.90	−120.90	sf	s	sf	23.55	22.24	20.45	1.31	1.80	3.10
6		−80.30	−112.80	s	g	g	23.74	23.34	21.49	0.40	1.85	2.26
7		2.00	−112.80	s	g	g	21.76	20.85	19.71	0.91	1.14	2.05
8		2.00	−107.60	s	sf	sf	21.85	21.09	20.28	0.75	0.82	1.57
9		80.90	−105.90	g	g	g	22.47	22.29	22.02	0.18	0.27	0.45
10		−73.40	−102.10	s	g	g	23.22	22.53	22.14	0.69	0.39	1.08
11		126.20	−100.90	s	sf	s	19.58	18.43	16.99	1.14	1.44	2.58
12		82.10	−98.00	g	g	g	21.52	20.71	19.77	0.81	0.94	1.75
13		16.20	−97.40	s	g	s	23.79	22.17	21.39	1.62	0.78	2.40
14		114.80	−96.30	s	s	g	24.49	23.94	21.69	0.55	2.25	2.80
15		−71.00	−96.00	g	g	sf	23.23	21.65	20.75	1.58	0.90	2.48
16		19.40	−94.50	sf	s	sf	23.59	23.30	22.20	0.29	1.10	1.39
17		82.90	−93.70	g	g	g	20.64	20.33	19.83	0.30	0.50	0.80
18		102.40	−91.90	s	g	g	23.61	21.95	20.28	1.66	1.68	3.33
19		−47.80	−90.50	g	g	g	21.38	20.33	19.51	1.05	0.81	1.87
20		87.00	−83.50	g	g	g	23.41	23.16	21.05	0.25	2.11	2.36
21		−75.70	−83.20	s	g	s	23.68	22.16	21.68	1.52	0.48	2.01
22		−86.10	−82.10	s	g	s	24.43	22.71	21.58	1.73	1.12	2.85
23		−37.10	−73.10	s	g	s	24.26	24.12	21.83	0.15	2.29	2.44
24		105.90	−67.60	s	sf	s	19.79	19.06	18.59	0.73	0.48	1.20
25		29.30	−68.40	s	g	s	23.55	23.20	21.60	0.36	1.60	1.96
26		−15.40	−66.40	g	g	g	22.98	21.87	21.11	1.10	0.76	1.86
27		−6.40	−56.00	s	g	g	24.13	21.59	20.65	2.55	0.94	3.49
28		24.40	−53.10	g	g	g	23.30	21.76	20.33	1.55	1.42	2.97
29		−68.40	−52.20	s	g	s	23.01	23.07	22.76	−0.06	0.31	0.25
30		−0.90	−51.00	g	g	g	23.86	23.27	21.35	0.59	1.92	2.51
31		−76.60	−50.50	g	g	g	22.27	21.85	21.11	0.42	0.74	1.17
32		−29.00	−49.30	g	g	g	21.75	20.34	19.41	1.40	0.93	2.33
33	H	−11.30	−47.80	g	g	g	21.00	19.90	19.03	1.10	0.88	1.97
34		−18.30	−47.00	g	g	g	22.79	21.80	21.11	0.98	0.69	1.67
35		−44.10	−46.40	s	g	s	23.53	22.33	21.47	1.20	0.86	2.05
36	F1	−33.10	−45.80	g	g	g	20.43	19.29	18.45	1.14	0.84	1.98
37		71.00	−44.70	g	g	g	21.52	20.41	19.58	1.10	0.83	1.93
38		107.30	−44.70	g	s	sf	24.00	22.81	20.99	1.19	1.82	3.01
39		18.30	−43.50	g	g	g	23.54	22.79	22.04	0.75	0.75	1.50
40		15.70	−40.00	s	s	g	23.26	22.51	21.58	0.76	0.93	1.68
41		106.40	−39.70	g	g	g	23.05	22.74	22.63	0.31	0.12	0.42
42		78.60	−39.40	s	s	g	23.52	22.91	21.54	0.62	1.36	1.98
43		−43.50	−37.70	g	s	s	23.95	22.73	22.09	1.22	0.64	1.86
44		17.70	−37.10	sf	s	sf	22.03	21.07	20.39	0.97	0.68	1.65
45	F2	−36.00	−37.10	g	g	g	21.33	19.77	18.78	1.56	1.00	2.55
46	D1	−7.50	−35.40	g	g	g	21.00	19.85	18.96	1.15	0.89	2.04
47		−29.90	−33.60	g	g	g	23.02	21.18	20.25	1.84	0.94	2.77
48		−81.50	−33.60	g	g	g	22.58	21.78	20.71	0.80	1.07	1.87
49		22.60	−33.60	g	g	g	23.15	21.81	21.62	1.34	0.19	1.53
50		85.00	−32.20	g	g	g	23.07	21.97	20.95	1.10	1.02	2.12
51	D2	−5.50	−29.60	g	g	g	21.04	19.99	19.24	1.05	0.76	1.81
52	A1	28.40	−26.10	g	g	g	20.28	19.29	18.48	0.98	0.82	1.80
53	A2	30.70	−22.60	g	g	g	20.41	19.31	18.45	1.10	0.86	1.97
54		107.30	−20.30	s	s	g	24.11	22.73	21.87	1.38	0.85	2.23
55		19.70	−18.60	g	g	g	23.69	22.14	22.08	1.55	0.05	1.61
56		−10.40	−18.60	s	g	s	23.02	22.39	22.28	0.63	0.11	0.74
57		−33.30	−17.70	s	g	s	23.55	21.81	20.62	1.74	1.19	2.93
58	B1 (star?)	12.20	−16.00	s	g	s	20.27	19.11	17.90	1.17	1.21	2.37
59		118.30	−15.70	g	g	g	20.50	19.57	18.70	0.93	0.87	1.80
60	B2	17.40	−12.80	g	g	g	20.40	19.24	18.40	1.17	0.84	2.01
61		23.80	−11.00	s	s	sf	23.20	22.10	21.27	1.10	0.83	1.93
62		88.50	−10.70	s	g	g	24.02	22.62	22.02	1.40	0.60	2.00
63		−51.90	−8.40	s	g	g	22.37	21.26	20.01	1.11	1.25	2.36
64		71.90	−4.30	s	s	g	23.67	23.04	22.39	0.63	0.66	1.29
65	BL Lac Total	−0.00	−0.00	s	sf	s	17.21	16.64	16.14	0.57	0.50	1.07
65a	BL Lac E-gal	−0.00	−0.00	g	g	g	19.05	17.95	16.52	1.07	0.97	2.04
66		107.90	−0.00	g	g	g	21.58	20.48	19.64	1.10	0.84	1.94

Table 4 (a) – *continued*

Obj	Notes	arcsec(E)	arcsec(N)	cl$V$	cl$R$	cl$I$	V	R	I	$V-R$	$R-I$	$V-I$
67		−46.70	1.40	g	g	g	24.11	22.62	21.91	1.49	0.71	2.20
68		92.80	1.20	g	sf	g	23.26	22.50	21.36	0.77	1.14	1.90
69	E1	30.20	3.80	g	g	g	21.09	20.14	19.32	0.95	0.83	1.78
70		87.00	4.10	g	sf	g	23.47	22.30	21.66	1.16	0.65	1.81
71	E2	98.00	4.40	g	g	g	21.78	21.12	20.37	0.66	0.75	1.41
72		28.70	4.90	g	g	g	20.91	20.00	19.23	0.90	0.77	1.68
73		75.40	6.40	s	g	g	24.05	21.71	20.44	2.34	1.27	3.61
74		67.90	9.90	g	g	g	21.53	20.94	20.29	0.58	0.65	1.23
75		75.70	9.60	g	g	g	23.16	21.57	20.48	1.59	1.09	2.68
76		−66.40	10.40	g	g	g	20.80	19.67	18.80	1.12	0.87	1.99
77		−6.40	11.60	sf	sf	s	22.24	21.07	20.28	1.16	0.80	1.96
78	C2	−20.60	18.60	g	g	g	21.04	20.08	19.24	0.96	0.84	1.79
79	C1	−26.10	18.60	g	g	g	20.36	19.45	18.64	0.91	0.81	1.72
80		126.10	20.00	g	s	g	23.41	22.38	21.60	1.03	0.77	1.81
81		56.50	21.20	g	g	g	22.32	21.34	20.59	0.99	0.75	1.74
82		106.10	21.80	sf	g	g	23.25	22.62	21.83	0.64	0.79	1.43
83		120.60	22.00	g	s	s	22.77	21.80	20.79	0.97	1.01	1.98
84	G ($z = 0.1$)	73.40	23.20	g	g	g	17.96	17.28	16.64	0.69	0.64	1.33
85		−24.90	23.80	g	s	g	23.60	22.99	21.27	0.61	1.72	2.34
86		−57.10	23.50	g	g	g	23.37	22.00	21.76	1.37	0.24	1.61
87		−85.30	25.20	g	g	g	21.41	20.99	20.46	0.42	0.54	0.95
88		27.80	25.80	g	s	s	23.20	22.34	21.97	0.85	0.37	1.23
89		−51.90	34.20	g	g	g	20.91	19.85	18.90	1.06	0.95	2.01
90		68.70	36.00	g	g	g	20.50	19.44	18.61	1.07	0.82	1.89
91		51.60	36.50	g	s	g	23.11	21.95	21.26	1.17	0.68	1.85
92		65.50	38.30	g	g	g	22.08	21.25	20.57	0.82	0.68	1.50
93		76.80	41.80	s	sf	s	20.26	19.38	18.72	0.88	0.66	1.54
94		13.60	44.90	g	s	g	23.73	22.98	22.24	0.75	0.75	1.49
95		47.80	48.40	g	g	g	20.61	19.80	19.12	0.81	0.67	1.49
96		111.40	49.00	g	g	g	22.64	21.61	20.83	1.03	0.78	1.81
97		109.30	55.10	s	sf	sf	23.34	22.34	21.13	1.00	1.21	2.21
98		−34.20	56.00	g	g	g	22.07	21.20	20.43	0.87	0.77	1.64
99		97.40	56.30	g	g	g	22.91	22.36	21.53	0.55	0.82	1.37
100		27.30	58.30	g	g	g	23.38	22.58	21.22	0.80	1.36	2.16
101		64.70	61.20	g	g	g	23.32	22.86	21.72	0.45	1.14	1.60
102		−70.20	62.60	s	g	s	20.53	19.69	18.89	0.84	0.80	1.64
103		−11.00	64.40	s	g	g	23.29	22.17	21.51	1.12	0.67	1.78
104		98.60	67.00	g	g	g	23.52	22.02	21.33	1.50	0.69	2.19
105		69.90	71.10	g	g	g	22.05	21.53	21.17	0.52	0.36	0.88
106		33.60	71.10	g	g	g	23.34	21.58	21.07	1.76	0.51	2.27
107		−54.80	71.60	g	s	s	22.49	21.74	21.09	0.75	0.65	1.40
108		−60.60	75.10	s	s	g	23.69	23.61	22.12	0.07	1.50	1.57

Table 4. (b) Objects classified as stars in the field surrounding the BL Lac H0414+009.

Obj	Notes	arcsec(E)	arcsec(N)	cl$V$	cl$R$	cl$I$	V	R	I	$V-R$	$R-I$	$V-I$
1		59.50	−86.70	s	s	s	23.94	23.55	23.20	0.39	0.35	0.75
2		20.90	−82.10	s	s	s	22.25	21.07	19.10	1.17	1.98	3.15
3		−56.30	−63.50	s	s	s	23.98	23.59	21.99	0.39	1.60	1.99
4		127.90	−56.00	s	s	s	18.87	17.97	17.35	0.90	0.62	1.52
5		11.30	−51.30	s	s	s	21.09	19.98	18.27	1.11	1.71	2.82
6		90.80	−42.30	s	s	s	17.17	16.41	15.88	0.76	0.54	1.30
7		−62.40	−38.60	s	s	s	23.03	21.87	20.98	1.16	0.89	2.06
8		21.70	−27.00	s	s	s	22.61	21.65	21.14	0.96	0.51	1.47
9		−13.30	−17.10	s	s	s	23.84	23.21	22.04	0.63	1.17	1.79
10		72.80	3.50	s	s	s	24.29	23.69	23.46	0.60	0.23	0.83
11		−68.70	4.30	s	s	s	21.85	20.74	19.17	1.11	1.58	2.68
12		−87.60	13.60	s	s	s	23.68	22.93	22.07	0.75	0.86	1.61
13		120.30	13.90	s	s	s	23.67	22.48	21.32	1.18	1.16	2.34
14		−65.00	33.90	s	s	s	23.59	23.31	22.54	0.28	0.77	1.05
15		115.10	43.80	s	s	s	19.58	18.85	18.37	0.73	0.48	1.21

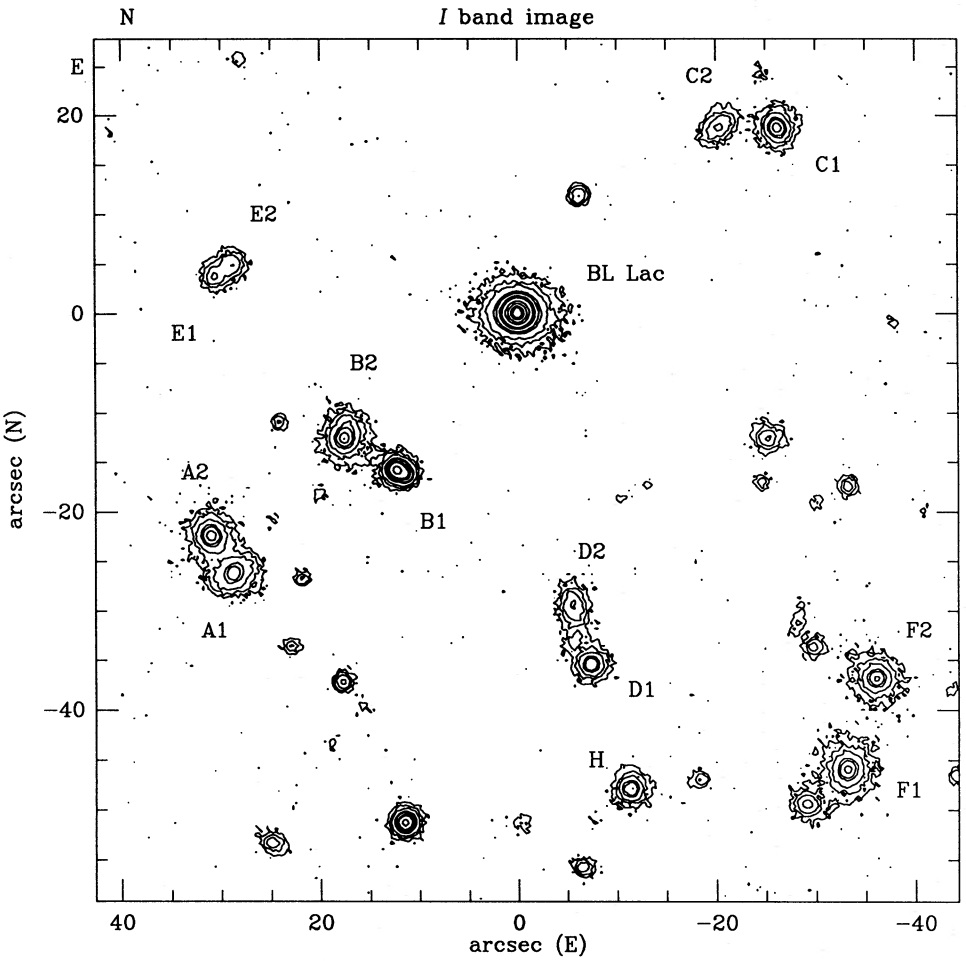

Figure 5. *I*-band contour map of the core of 0414+009 showing the galaxy pairs labelled as in Falomo *et al.* (1991). The individual galaxy properties are listed in Tables 4 and 5.

apparent pairs are actually the result of lensing by a cosmic string, that string would have to have a very contorted morphology.

We would expect lensed twin galaxies to have similar colours and magnitudes. However, the colours and magnitudes for the six pairs are not very similar. They are listed separately in Table 5. The morphologies of the individual galaxies in the pairs also contradict the lensing hypothesis. None of the so-called twin galaxies (except maybe E1 and E2) actually looks like its twin. B1 is probably a star. It is classified as a galaxy in the *R* image only, and inspection of the *I* contour plot shows a centrally peaked round object with a slight extension. B2 is very different and is definitely a galaxy. A1 is clearly elongated SE–NW and has a lower central surface brightness than A2; C1 has a brighter core than C2 which is also elongated SE–NW; and D1 is brighter and more compact and circular than D2.

The Abell richness of 0414+009 can be measured by counting the number of galaxies within a 3-Mpc radius in the magnitude range m_3 and m_3+2 (where m_3 is the magnitude of the third-ranked cluster galaxy). Unfortunately it is quite difficult to determine this richness, since our CCD field only covers a ~0.6-Mpc radius around the BL Lac. If we count all the galaxies in the CCD field (i.e. those objects which are classified as galaxies in all three colours) within this magnitude range, we obtain 34 galaxies. However, 15 of these are probably field galaxies (Tyson 1988), resulting in $N(<m_3+2)\simeq 16$. When we correct for the limited field of view of the CCD, following Luppino *et al.* (1991), we are able to scale this number back to roughly 31 galaxies within the standard Abell radius, thus making this cluster Abell richness class 0. Needless to say, the final richness estimate is somewhat uncertain.

Our magnitudes also allow us to classify the cluster under the Bautz–Morgan classification scheme (Bautz & Morgan 1970). Dressler (1978) quantifies this scheme in terms of $\Delta=(m_2-m_1)+(m_3-m_1)$, where m_1, m_2 and m_3 are the magnitudes of the first-, second- and third-ranked cluster galaxies and correspond here to the BL Lac host galaxy itself ($m_1=19.10$ in the *V* band), A1 ($m_2=20.28$) and F1 ($m_3=20.43$). We ignore B1 as it is probably a star. In the Dressler scheme, BM I clusters have $\Delta\geq 2.25$, BM II clusters have $1.03\leq\Delta\leq 2.25$, and BM III clusters have $\Delta\leq 1.03$. For this cluster we find $\Delta=2.56$ (in the *V* band), classifying it as BM I. HGT also give the absolute magnitudes of the brightest cluster galaxies (BCGs) in the various BM classes. HGT find $\langle M_V\rangle_{\rm BCG}=-23.32\pm0.27$ for BM I clusters, -23.20 ± 0.28 for BM II clusters and -22.91 ± 0.28 for

Table 5. Spectroscopy of 0414+009 and some surrounding galaxies.

Name	Obj	z	class	V	R	I	$V-R$	$R-I$	Comments
BL Lac	65	0.287	g	17.21	16.64	16.14	0.57	0.50	CaII H and K, MgIb, TiO
A1	52		g	20.28	19.29	18.48	0.98	0.82	
A2	53		g	20.41	19.31	18.45	1.10	0.86	no features in spectrum
B1	58		s?	20.27	19.11	17.90	1.17	1.21	looks like a star
B2	60	0.287	g	20.40	19.24	18.40	1.17	0.84	CaII
C1	79	0.289	g	20.36	19.45	18.64	0.91	0.81	CaII
C2	78		g	21.04	20.08	19.24	0.96	0.84	
D1	46	0.276	g	21.00	19.85	18.96	1.15	0.89	CaII, H_β, FeI, [SII]?
D2	51		g	21.04	19.99	19.24	1.05	0.76	no features in spectrum
E1	69		g	21.09	20.14	19.32	0.95	0.83	
E2	71		g	21.78	21.12	20.37	0.66	0.75	
F1	36	~ 0.28	g	20.43	19.29	18.45	1.14	0.84	MgIb?
F2	45		g	21.33	19.77	18.78	1.56	1.00	
H	33	0.277	g	21.00	19.90	19.03	1.10	0.88	CaII, [SII]?
G	84	0.101	g	17.96	17.28	16.64	0.69	0.64	H_α and H_β

BM III clusters. Thus the host of 0414+009 is more consistent with being the BCG in a BM II or III cluster. However, we must remember that the value of Δ is the primary classification criterion and the absolute magnitudes are derived thereafter. Also, the absolute magnitude decreases (i.e. the galaxy gets brighter) with increasing richness, and the cluster here is not particularly rich. We therefore conclude that the host galaxy of 0414+009 is the brightest galaxy in a cluster of $R \leq 0$ and probably of BM class I.

3.2 Spectral observations – the physical reality of the apparent cluster

In order to determine whether the apparent cluster is a real physical association or just a chance line-of-sight superposition of galaxies, we made spectral observations of a number of objects in the field, including the BL Lac itself. A log of the spectroscopic observations using both the Mitchigan–Dartmouth–MIT (MDM) 2.4-m telescope and the Anglo–Australian Telescope (AAT) is given in Table 2 at the beginning of this section. The results of the spectroscopy are listed in Table 5.

Most of the spectroscopic observations were carried out on the 2.4-m Hiltner telescope of the MDM Observatory on Kitt Peak. We used the MkIII spectrograph with a 300 lines mm^{-1} grism and a Thomsen 576 × 384-pixel CCD. The wavelength range was set roughly from 4300 to 7300 Å with a dispersion of 5.14 Å $pixel^{-1}$ and a resolution of approximately 11 Å. We used two slits (2.4 and 1.7 arcsec) for these observations. the location and position angle (PA) of the long slit was set such that each orientation passed through the BL Lac. (We use the standard definition of position angle, i.e. PA 0° corresponds to north–south and positive angles correspond to anticlockwise or easterly rotations.) Five 1200-s exposures were taken with the slit orientated at PA 72°.7, thus picking up galaxy G to the north-east. Two 1200-s exposures and one 836-s exposure were acquired with the slit in PA 126°, covering objects A2, B2 and C1, and three 1200-s exposures and one 1800-s exposure were taken with the slit in PA 13°, covering objects D2, D1 and H. All of the above spectra were taken under photometric conditions. Additional observations of the spectrophotometric standards PG0216+032, Feige 110 and Feige 34 were acquired to flux calibrate our spectra. The spectra were reduced in the usual way.

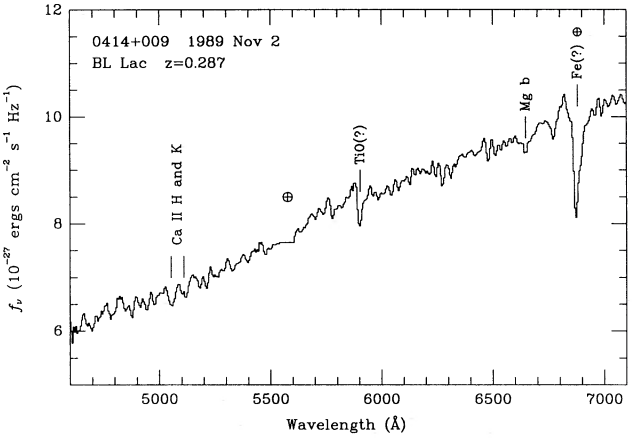

Figure 6. Spectrum of the BL Lac itself. Twelve separate exposures totalling 14 636 s were combined to produce this spectrum.

The composite spectrum of the BL Lac assembled from all of the above individual spectra (total integration time 14 636 s) is shown in Fig. 6. This spectrum has been smoothed with a two-pixel Gaussian. We can identify absorption features of Ca II *H* and *K*, TiO (4583 Å) and Mg I *b*. These features are characteristic of an elliptical or S0 galaxy at a redshift of $z = 0.287$, confirming the redshift determination of Halpern *et al.* (1991). The deep absorption feature near 6800 Å is the atmospheric *B* band. Unfortunately, Fe I would lie at this redshift and a weak Fe I feature is also present in the spectrum shown by Halpern *et al.* (1991). In Fig. 7

we present the spectrum of object G, the bright galaxy to the north-east of the BL Lac. Clearly this is a foreground object with $z = 0.101$, based on the identification of Hα and Hβ emission lines. As mentioned above, spectra of six of the fainter galaxies surrounding the BL Lac were also acquired. Four of these spectra are shown in Fig. 8. Objects B2, C1, D1 and H all appear to be galaxies at roughly the same redshifts as the BL Lac (although some of the line identifications are admittedly a bit uncertain – especially for object C1). The spectra for objects A2 and D2 had no believable features, and are not shown.

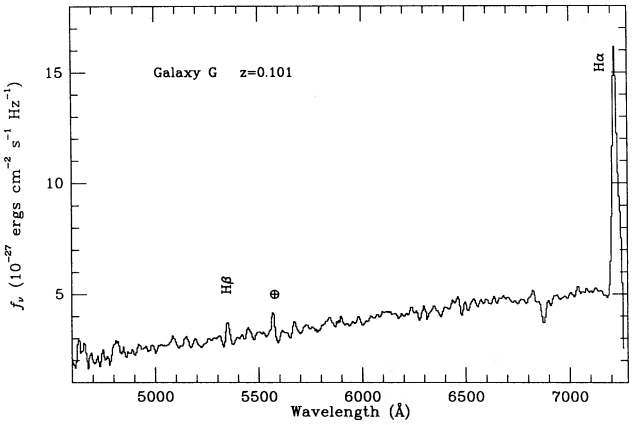

Figure 7. Spectrum of the $z = 0.101$ bright elliptical galaxy north-east of BL Lac (galaxy G).

The spectral observations on the AAT were taken with the FORS and with the IPCS under conditions of intermittent slight clouds. Nothing was detected in the two 1800-s IPCS observations. In the FORS observations, a long slit was placed at PA 57°, centred on galaxy B2. The slit also covered objects B1, D2, F1 and G (the slit did not cover the BL Lac in these observations). Two 1800-s spectra were taken. The wavelength range extended from 5150 to 11 080 Å at a scale of 10.1 Å per channel. The spectral resolution was approximately 20 Å. Night sky features were removed using observations of the relatively featureless star HD 2796. Galaxy G was again easily detected and a redshift of 0.1008 ± 0.0002 measured from Hα/N II and [S II], confirming the MDM result above. Galaxies B2, B1, D2 and F1 were all detected at between 5 and 10 per cent of the sky brightness. None showed emission lines and no believable absorption features could be detected in objects B1 or D2. However, galaxies B2 and F1 both showed a wide absorption feature at ~6628 Å. If this is the Mg I *b* band, then the redshifts of both galaxies are ~0.28.

Thus five galaxies have redshifts similar to that of the BL Lac host, confirming the physical reality of the cluster.

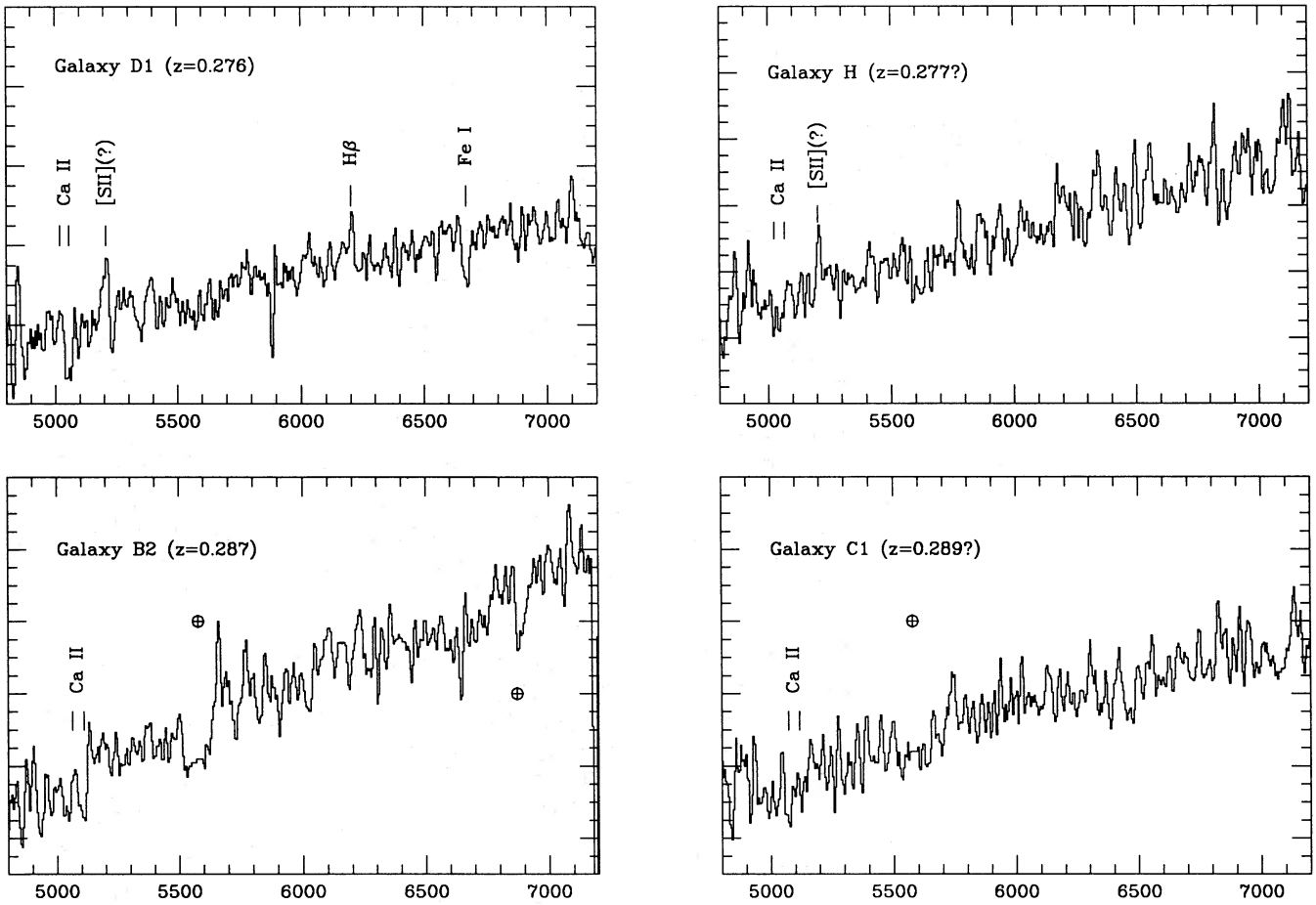

Figure 8. Spectra of four of the faint galaxies (B2, C1, D1 and H) surrounding the BL Lac.

4 X-RAY OBSERVATIONS – A SEARCH FOR EXTENDED EMISSION FROM AN INTRACLUSTER MEDIUM

Given the physical reality of the cluster of galaxies surrounding 0414+009, and the bent tail-like morphology of the radio source, one might suspect the presence of hot intracluster gas. We note that Ulmer *et al.* (1983) state that the X-ray image of 0414+009 is unresolved ($\leq$3 arcsec) in *Einstein* HRI observations. They do not state whether they searched for any very faint extended surrounding structure. 0414+009 was also observed on four occasions separated by about a week each in 1984 September by the *European X-ray Astronomy Satellite* (*EXOSAT*). The X-ray spectral variability of the BL Lac core is fully detailed by George (1988) and Giommi *et al.* (1990) and is not described here. However, we have carried out a careful search of the deep *EXOSAT* LE images for possible extended emission and we present the results here.

Judging from the approximate size of the cluster on the CCD images, <2 arcmin, we expect, by comparison with nearby clusters, any extended emission to be not larger than about 1 arcmin in diameter, and possibly much smaller. We therefore searched for emission on this scale, quite near the BL Lac. The four LE images were rotated on the same roll angle (there are only a few degrees difference between them) and summed. We then derived a radial profile. There are no other sources, which could contaminate the profile, visible in the field of view (a 10σ upper limit on any such unresolved source is 0.0036 count s^{-1}).

Any extended emission near 0414+009 will be masked, to some extent, by the wings of the point response function to 0414+009 which must therefore first be subtracted. As the point response function varies with energy, and hence with the source spectrum, its best estimate for 0414+009 is ideally given by that of a bright isolated BL Lac source. Here we use a 1-day observation of the isolated BL Lac Mkn 501, which is roughly 10 times brighter than 0414+009. We therefore derived the radial profile for Mkn 501 and scaled it in intensity until the best fit was obtained between it and the 0414+009 radial profile. As we are interested in searching for possible extended emission surrounding 0414+009, we restricted the fitting procedure to the inner 6 pixels (22 arcsec) of the radial profile. The best fit (which required scaling the Mkn 501 profile by 0.083) produced a reduced χ^2 of 0.64. At larger radii, the scaled Mkn 501 profile continued to fit very well within the errors, in all cases, to that of 0414+009. We therefore find no evidence for extended emission near 0414+009. From consideration of the errors we conclude that an upper limit to any extended emission in a region of 70-arcsec radius surrounding 0414+009 is 1×10^{-3} count s^{-1}. We adopt this value as an upper limit to the emission from the surrounding cluster.

At a redshift of $z=0.287$ with a galactic obscuring column of 8×10^{20} cm^{-2} (Stark *et al.*, in preparation), and assuming a thermal bremsstrahlung spectrum with a temperature of 2 keV, these observations correspond to an upper limit on the luminosity of 4×10^{44} erg s^{-1} (2–10 keV). For an assumed temperature of 4 keV, this luminosity drops by a factor of 2, but still corresponds to a reasonably luminous cluster X-ray source, of sufficient density (under any reasonable assumptions) to affect the morphology of the radio-tail source.

5 CONCLUSIONS

We have presented detailed radio, optical and X-ray observations of the X-ray selected BL Lac 0414+009. We find that it exhibits a large, curved steep-spectrum radio jet or tail extending from the BL Lac core to the east. There is no evidence of extended radio emission to the west, so the jet is intrinsically single sided. The luminosity and structure of the tail are consistent with a FR I classification and strengthen the association of BL Lacs with this type of radio source. This is the first time a large, single-sided radio tail or jet has been seen associated with a BL Lac. The tail structure has some similarities to that of radio sources found in nearby clusters of galaxies.

We present deep, multicolour CCD images and spectra that confirm that the BL Lac host galaxy is the brightest member of a BM I cluster which may be as rich as Abell richness class 0. From its surface brightness profile and colours, we conclude that the host galaxy of the BL Lac 0414+009 is most likely an elliptical galaxy. We confirm the redshift for the BL Lac measured by Halpern *et al.* (1991) and calculate an absolute total magnitude of $M_V=-23.53$. We have also obtained redshifts of other galaxies in the field. Five of these have redshifts similar to that of the BL Lac. The apparent cluster is therefore a real physical association and not a chance superposition of galaxies.

We have carefully examined the hypothetical 'twin' galaxies and conclude that there is no compelling evidence for lensing by a cosmic string as proposed by Falomo *et al.* (1991).

We have searched deep *EXOSAT* images for extended X-ray emission that might be produced from hot intracluster gas. We find none, but the upper limit to the cluster X-ray emission [L_x(2–10 keV)$\leq4\times10^{44}$ erg s^{-1}], is comparable to that from moderately luminous Abell clusters, and the implied hot gas could still be responsible for the distorted shape of the radio tail.

Our observations conflict with the hypothesis that BL Lacs avoid the cluster environment (Weistrop *et al.* 1981). On the contrary, evidence is gradually accumulating for an alternative proposition that BL Lacs are found in groups or clusters just as frequently as are normal radio galaxies, i.e. in about 20 per cent of cases for Abell-type clusters and even more often for poor groups (e.g. M^{c}Hardy 1979). Additional examples of BL Lacs in clusters include 3C66A (Butcher *et al.* 1976), 1400+162 (Weistrop *et al.* 1983), H1100−230 (=3A1057−224) and H1430+423 (=3A1422+425) (Remillard *et al.* 1989).

It is not surprising that clusters surrounding BL Lacs have not been discovered until recently. Most BL Lacs are too distant for surrounding cluster galaxies to be easily visible on the Palomar or UK Schmidt sky surveys (e.g. Burbidge & Hewitt 1987). Now that deep CCD images are being acquired for more and more BL Lacs, many of the faint galaxies in surrounding clusters are emerging. The present statistics do not, of course, allow us to confirm this hypothesis, but in the light of the presently popular 'unified scheme' for AGN (e.g. Browne 1989) we suggest that this hypothesis has the soundest physical basis and that it henceforth be taken as the default hypothesis. All observers suggest that the groups surrounding the various BL Lacs are not rich. This is entirely consistent with the above hypothesis, as many more

radio sources appear in poor groups than in rich clusters which, in turn, is merely a reflection of the fact that there are many more poor groups than rich clusters. For radio sources in general, it has been shown that the frequency of appearance of a radio source in a cluster is not a function of the cluster environment, but is almost entirely a function of the absolute magnitude of the host galaxy (McHardy 1979). Once in existence, however, the resultant radio source can be significantly affected by the cluster environment. It appears that the same thing has happened in the case of 0414 + 009. The continuum source has similar properties to other BL Lac sources, but the beam may be deflected by the intracluster medium producing the radio tail which we see.

ACKNOWLEDGMENTS

We thank Bob Warwick and Gordon Bromage for their interests and efforts at an early stage of this project. We also thank the US National Radio Astronomy Observatory for observing time on the Very Large Array and the Massachusetts Institute of Technology for observing time on the 2.4-m Hiltner Telescope. We thank the Anglo–Australian Observatory for service observations on the Anglo–Australian Telescope and Robert Jedrzejewski for his profile-fitting software. IMG acknowledges the SERC for a postgraduate studentship.

REFERENCES

Abraham, R. G., 1991. *DPhil thesis,* Oxford University.
Abraham, R. G., McHardy, I. M. & Crawford, C. S., 1991. *Mon. Not. R. astr. Soc.,* **252,** 482.
Antonucci, R. R. J. & Ulvestad, J. S., 1984. *Nature,* **308,** 617.
Bautz, L. P. & Morgan, W. W., 1970. *Astr. J.,* **162,** L149.
Browne, I., 1989. In: *BL Lac Objects,* p. 401, eds Maraschi, L., Maccacaro, T. & Ulrich, M.-H., Springer-Verlag, Berlin.
Burbidge, G. & Hewitt, A., 1987. *Astr. J.,* **92,** 1.
Butcher, H. R., Oemler, A., Tapia, S. & Terenghi, M., 1976. *Astrophys. J. Lett.,* **209,** L11.
Cawson, M., 1983. *PhD thesis,* Cambridge University.
Colla, G., Fanti, C., Fanti, R., Gioia, I., Lari, C., Lequeux, J., Lucas, R. & Ulrich, M. H., 1975. *Astr. Astrophys.,* **38,** 209.
Cowie, L. & Hu. E., 1987. *Astrophys. J. Lett.,* **318,** L33.
Dressler, A., 1978. *Astrophys. J.,* **222,** 23.
Elvis, M., Lockman, F. J. & Wilkes, B. J., 1989. *Astr. J.,* **97,** 777.
Falomo, R. & Tanzi, E. G., 1991. *Astr. J.,* **102,** 1294.
Falomo, R., Melnick, J. & Tanzi, E. Q., 1990. *Nature,* **345,** 692.
Falomo, R., Tanzi, E. G. & Treves, A., 1991. Preprint.
Fanaroff, B. L. & Riley, J. M., 1974. *Mon. Not. R. astr. Soc.,* **167,** 31P.
George, I. M., 1988. *PhD thesis,* Leicester University.
Giommi, P., Barr, P., Garilli, B., Gioia, I. M., Maccacaro, T., Maccagni, D. & Schild, R. E., 1990. *Astrophys. J.,* **356,** 432.
Halpern, J. P., Chen, V. S., Madejski, G. M. & Chanan, G. A., 1991. *Astr. J.,* **101,** 818.
Hintzen, P. & Owen, F., 1981. *Astr. J.,* **86,** 1577.
Hoessel, J. G., Gunn, J. E. & Thuan, T. X., 1980. *Astrophys. J.,* **241,** 486 (HGT).
Jarvis, J. F. & Tyson, J. A., 1981. *Astr. J.,* **86,** 476.
Jedrzejewski, R. I., 1987. *Mon. Not. R. astr. Soc.,* **226,** 747.
Landolt, A., 1983. *Astr. J.,* **88,** 439.
Luppino, G. A., 1989. *PhD thesis,* Massachusetts Institute of Technology.
Luppino, G. A., Cooke, B. A., McHardy, I. M. & Ricker, G. R., 1991. *Astr. J.,* **102,** 1.
McHardy, I. M., 1979. *Mon. Not. R. astr. Soc.,* **188,** 495.
McHardy, I. M., Marscher, A. P., Gear, W. K., Muxlow, T., Lehto, H. J. & Abraham, R. G., 1990. *Mon. Not. R. astr. Soc.,* **246,** 305.
McHardy, I. M., Abraham, R. G., Crawford, C. S., Ulrich, M.-H., Mock, P. C. & Vanderspek, R. K., 1991. *Mon. Not. R. astr. Soc.,* **249,** 742.
Ostriker, J. P. & Vietri, M., 1985. *Nature,* **318,** 446.
Ostriker, J. P. & Vietri, M., 1990. *Nature,* **344,** 45.
Remillard, R. A., Tuohy, I. R., Brissenden, J. V., Buckley, D. A. H., Schwartz, D. A., Feigelson, E. & Tapia, S., 1989. *Astrophys. J.,* **345,** 140.
Rusk, R., 1988. In: *The Impact of VLBI on Astrophysics and Geophysics,* p. 161, eds Reid, M. J. & Moran, J. M., Kluwer, Dordrecht.
Schmelz, J. T., Feigelson, E. D. & Schwartz, D. A., 1986. *Astr. J.,* **92,** 585.
Tyson, J. A., 1988. *Astr. J.,* **96,** 1.
Ulmer, M. P., Brown, R. L., Schwartz, D. A., Patterson, J. & Cruddace, R. G., 1983. *Astrophys. J. Lett.,* **270,** L1.
Ulmer, M. P. *et al.,* 1980. *Astrophys. J.,* **235,** 351.
Ulrich, M.-H., 1989. In: *BL Lac Objects,* p. 45, eds Maraschi, L., Maccacaro, T. & Ulrich, M.-H., Springer-Verlag, Berlin.
Wardle, J. F. C., Moore, R. L. & Angel, J. R. P., 1984. *Astrophys. J.,* **279,** 93.
Weistrop, D., Shaffer, D. B., Reitsema, H. J. & Smith, B. A., 1983. *Astrophys. J.,* **271,** 471.
Weistrop, D., Shaffer, D. B., Mushotsky, F., Reitsema, H. J. & Smith, B. A., 1981. *Astrophys. J.,* **249,** 3.